JOURNAL OF MECHANICS OF CONTINUA AND MATHEMATICAL SCIENCES
www.journalimcms.org

ISSN (Online) : 2454 -7190 Vol.-21, No.-02, February (2026) pp 106-124 ISSN (Print) 0973-8975

GRAPHENE OXIDE-MODIFIED SLAG CEMENT CONCRETE: EFFECTS ON MECHANICAL STRENGTH, RESISTANCE UNDER AGGRESSIVE ENVIRONMENTS AND MICROSTRUCTURE EVOLUTION

Saruk Mallick[1], Prasanna Kumar Acharya[2]

[1,2] School of Civil Engineering, Kalinga Institute of Industrial Technology (KIIT) Deemed to be University, Bhubaneswar, Odisha, India.

Email: [1]sarukmallick001@gmail.com; 2081053@kiit.ac.in
[2]pkacharya64@yahoo.co.in; prasanna.acharyafce@kiit.ac.in

Corresponding Author: **Prasanna Kumar Acharya**

https://doi.org/10.26782/jmcms.2026.02.00007

(Received: December 07, 2025; Revised: January 23, 2026; Accepted : February 04, 2026)

Abstract

This study investigated the influence of graphene oxide (GO) on enhancing the mechanical characteristics and microstructure of concrete made of slag cement. Concrete samples were made with and without GO, added in varying dosages from 0.01% to 0.1% by weight of cement. The mechanical performance of these specimens was evaluated through compressive, tensile, and flexural strength tests. The durability was checked through acid and sulphate attack tests. To ensure uniform dispersion of GO within the matrix, polycarboxylate ether-based superplasticizer was employed at a measure of 0.25% by weight of cement. Scanning electron microscopy (SEM) was conducted to observe the microstructural development, while energy-dispersive X-ray spectroscopy (EDX) and X-ray Diffraction (XRD) were used to check the composition of the elements of the GO-modified matrix and its contribution to concrete health. The study found that GO addition is beneficial in enhancing compressive, tensile, and flexural strength up to 61, 109, and 39% at 28 days in comparison with conventional concrete. The acid and sulphate resistance of GO-modified concrete was found to be 46% and 30% better than that of control concrete. The effect of GO up to 0.05% on the properties of concrete is found in an increasing trend. SEM analysis confirmed improved dispersion of GO and enhanced interfacial bonding with cement particles. The EDX and XRD analyses validated the macro-level results. These findings highlight the potential of GO as an effective nanomaterial for improving the performance of slag cement-based composites.

Keywords: Mechanical characteristics, Graphene oxide, Acid resistance, Sulphate resistance, Microstructure

I. Introduction

Carbon-based nanomaterials have been widely explored for enhancing the properties of cement composites. Several studies have reported significant improvements in both compressive and tensile strengths of cementitious composites upon the incorporation of small amounts of graphene oxide. Pan et al. [XXVII] observed increases of 15–33% in compressive strength and 41–59% in tensile strength with the addition of 0.05% GO in mortar. Similarly, Lv et al. [XXI, XXIII] demonstrated experimentally the effects of GO on the mechanical characteristics of both cement paste and mortar. Wang et al. [XXXIII] attributed such enhancements to the action between the carboxyl groups of GO and hydrates, which form a denser cementitious matrix. Further, GO has been shown to enhance durability aspects such as carbonation and freeze-thaw resistance, as demonstrated by Long and Mohammed et al. In addition, Gaitero et al. [XII] reported that GO nanoparticles (GONPs) influence cement hydration, promoting the formation of C–S–H crystals. Chuah et al. [IX] found that small amounts of GONPs increased the compressive strength of cement paste by approximately 46.2%. Beyond mechanical strength, Sedaghat et al. [XXX] observed a notable reduction in the electrical resistivity of concrete with GO addition. Liu et al. [XX] reported on the improvement of fracture toughness of cement paste on the inclusion of graphene sheets. Gholampour et al. [XIII] reported that the oxygen content of GO significantly affects the compressive strength of cement composites, with optimum performance achieved at a moderate degree of GO reduction. Meanwhile, Shang et al. [XXXII] noted that while the presence of silica fume might limit some pozzolanic reactions, it improves the mixing of GO in the cement system due to its physical shape effect, facilitating better distribution of GO.

Li et al. [XIX] indicated that incorporating 0.5% multiwalled carbon nanotubes (MWCNTs) led to significant improvements in both 28-day compressive and flexural strengths. Cwirzen et al. [XX]. Konsta-Gdoutos et al. [XVI] highlighted the importance of aspect ratio, noting optimal concentrations of up to 0.08 wt% for short MWCNTs and below 0.048 wt% for longer ones. Similarly, carbon nanofibers (CNFs) have been reported to enhance compressive, tensile, and flexural strengths in macrodefect-free (MDF) cement composites [XV]. Sáez De Ibarra et al. [XXVIII] investigated both single-walled and multi-walled CNTs dispersed in water with and without gum Arabic, observing that MWCNTs outperformed SWCNTs in enhancing Young's modulus and hardness, although the latter's straightness and dispersion challenges limited their effectiveness. Li et al. [XVII, XVIII] further improved the performance of MWCNTs through acid functionalization, achieving increases of 25.1% in flexural strength and 18.9% in compressive strength after 28 days of curing, with treated nanotubes outperforming untreated ones. Nasibulin et al. [XXVI] introduced an innovative method for growing CNTs directly on cement particles, resulting in over a cent percent increase in strength.

Shah et al. [XXXI] dispersed MWCNTs (0.02–0.33 wt%) using surfactants and ultrasonication, achieving notable improvements in mechanical properties, including 15–55% higher Young's modulus and 8–40% greater flexural strength, alongside a 30–40% decrease in autogenous shrinkage. Chaipanich et al.[VIII] reported approximately 10% improvements in compressive strength with 0.5–1% CNT

additions to fly ash cement. At the microstructural level, Makar [XXV] observed reinforcing effects such as crack bridging and fiber pullout in single-walled CNT composites. Authors [XXIX, XI] reported enhancements in compressive and flexural strength through the incorporation of CNFs and silica fume, although agglomeration affected performance. Kang et al. [XIV] highlighted the substantial benefits of nanographene oxide (GO), with 1% GO improving compressive strength by up to 63% after 28 days, and 0.03% GO increasing compressive and tensile strengths by 21.37% and 53.77%, respectively. Lv et al. [XXIV, XXIII] demonstrated through SEM analysis that GO promotes the formation of uniform, flower-like nanocrystals during cement hydration, contributing to enhanced toughness. Wang. et al. [XXXIV] found that GO addition enhanced compressive and indirect tensile strengths by 13.1% and 41.3%, respectively, at 28 days.

II. Research significance

The literature review indicates that most existing studies on the use of graphene oxide have focused primarily on ordinary Portland cement (OPC). However, the production of OPC involves significant consumption of natural resources, requires high amounts of non-renewable energy, and contributes substantially to carbon dioxide emissions. Consequently, the use of OPC is increasingly being discouraged. In contrast, cements like Portland slag cement (PSC), which utilize industrial by-products such as slag, are considered more sustainable alternatives. Therefore, the production and use of PSC are being actively encouraged. Despite this, research on the influence of GO on PSC-based concrete remains limited. An in-depth discussion on the strength development of GO reinforced concrete, specifically addressing the combined physical and chemical effects, is largely lacking in existing literature and still represents a significant research gap. The performance of GO-modified PSC-based concrete under aggressive environments is not well understood from the existing literature. Moreover, further studies are needed to better understand the microstructure and interfacial transition zone of GO-reinforced concrete. The present study aims to address these identified research gaps.

III. Experimental works

Materials

The experiment was conducted using the following materials.

Cement

The cement used in this research was Portland slag cement (PSC), according to IS 455–2015 [IV]. The physical characteristics of cement are listed in Tables 1 and 2.

Table 1: Physical properties of cement

Particulars	Results
Specific gravity	3.00
Standard consistency	32%
Fineness of cement	370 m^2/kg
Soundness Test	0.6 mm
Setting time (Initial)	162 min
Setting time (Final)	220 min

Table 2: Chemical properties of cement

Particulars	Results
Insoluble residue	0.37%
Magnesia	4.78%
Chloride	0.02%
Sulphuric anhydrite	2.58%
Sulphide sulfur	0.28%
Loss on ignition	1.66%

Aggregates

The river sand and locally available granite chips conforming to the requirements of IS 383 [III] were used as aggregates whose properties are listed in Table 3.

Table 3: Properties of fine and coarse aggregates

Features	Fine aggregates	Coarse aggregates
Bulk density	1655 kg/m^3	1694 kg/m^3
Fineness modulus	2.40	6.49
Grading size	<4.75 mm	<4.75 mm
Water absorption	0.84 %	0.22 %
Impact value		15.32%
Abrasion value		18.58%
Specific gravity	2.72	2.84

Graphene oxide

The GO used in this study had a purity greater than 99.8% and a surface area of 351 m^2/g, determined via nitrogen adsorption-desorption analysis. The spectroscopic characteristics of GO were examined using a Renishaw India Reflex micro-Raman spectrometer equipped with an Ar^+ ion laser. The Raman spectrum revealed three characteristic bands: G, D, and 2D. The G band, located at 1570 cm^{-1}, relates to the in-plane vibrations of sp^2 carbon networks (E_{2g} symmetry) at the Brillouin zone center. The D band, observed at 1345 cm^{-1}, arises from defects and edge disorder in the GO. The 2D band at 2693 cm^{-1} arises from second-order two-phonon processes involving in-plane vibrations near the K-point. The intensity ratio (I_G/I_2D) of 2.6 suggests the presence of 4–5 graphene layers in the GO. Additionally, the optical band gap of GO was measured by UV-Vis diffuse reflectance spectroscopy (Thermo Scientific Evolution 220), and the band gap energy was calculated as 4.69 eV using the Kubelka–Munk function. These results confirm the multi-layered structure and semiconducting nature of the GO used in this work.

Water

The water used in this study was portable type collected from the tap of the laboratory. The properties of water are listed in Table 4.

Table 4. Properties of water

Features	Results
pH value	7.0
Sulphates	76 mg/l
Suspended solids	0
Dissolved solids	292 mg/l
Chlorides	21mg/l
MPN value	0

Super plasticizer

A superplasticizer (SP) based on polycarboxylate ether was used at a dosage of 0.25% by weight of binder. The properties of SP are listed in Table 5.

Table 5. Properties of superplasticizer

Features	Results
pH value	6.45
Specific gravity	1.075
Volumetric mass	1.09 kg/l
Alkali	<1.5 g/l
Chlorides	<0.1%

Methods

To examine the effect of graphene oxide on the mechanical characteristics of cement concrete a mix design was prepared targeting M20 grade concrete following the guide lines of IS 10262 [II], specimens were prepared using a proportion of 1:2:4:0.45 (Binder: Fine aggregates: Coarse aggregates: Water) with varying GO dosages of 0.01, 0.02, 0.03, 0.04, 0.05 and 0.1% by weight of cement, along with a control mix without GO. The control mix containing 0% of GO was named as GOC0. Similarly, concrete mixes containing 0.01, 0.02, 0.03, 0.04, 0.05, and 0.1% of GO were named as GOC1, GOC2, GOC3, GOC4, GOC5, and GOC6. The quantity of PSC was 330 kg per one cubic meter of concrete. For each mix proportion, a minimum of three specimens was cast to ensure consistency and reliability of results across mechanical strength tests, including compressive, tensile, and flexural strength assessments. The specimens were prepared in standard shapes and sizes: cubes of 100 mm size for compressive strength, cylinders (100 mm diameter × 200 mm long) for tensile strength, and beams (100 mm × 100 mm × 500 mm) for flexural strength testing. All specimens were cured for 7, 14, and 28 days to evaluate the strength development over time. For the tests of compressive strength and flexural strength, the guidelines of IS 516 (Part 1/Sec 1) [V] and IS 516 (Part 2/Sec 2) [VI] were followed. Similarly, for the test of splitting tensile strength, the guidelines of IS 5816 [VII] were followed. For the tests of acid and sulphate resistance, the procedure as reported in the past publication [I] was followed. For these tests, 28-day water-cured concrete samples were immersed in 1% sulphuric acid and 1% magnesium sulphate solution for further 28 days. After this period, the samples were subjected to compressive strength tests.

The strength loss was computed by comparing the strength of water-cured samples of the same age.

IV. Results and discussions

Compressive strength

Figure 1 presents the details of compressive strength tests for concrete samples containing varying percentages of graphene oxide at curing intervals of 7, 14, and 28 days. The control sample (GOC0) exhibited compressive strengths of 16.68 MPa, 20.53 MPa, and 24.74 MPa at 7, 14, and 28 days, respectively. In contrast, all GO-modified samples showed noticeable improvements in strength at each curing period. A clear trend of strength enhancement is observed with the incremental addition of GO from 0.01% to 0.05% and 0.1%. The improvements in compressive strength of GOC1, GOC2, GOC3, GOC4, GOC5, and GOC6 at 28 days, compared to the control (GOC0), are found to be 16, 22, 32, 43, 61, and 19 %. The data clearly indicate a progressive increase in compressive strength with higher GO content up to 0.05%. At 0.05% GO (GOC5), the compressive strength improved by approximately 61 % compared to the control sample. At 0.1 % GO content, a drop in strength occurs due to GO agglomeration, reduced dispersion, and microvoid formation. However, the strength remains over the normal concrete.

The observed improvement in compressive strength with increasing GO dosage can be attributed to the following mechanisms: (a) Graphene oxide acts as a heterogeneous nucleation site during the hydration of cement, facilitating the formation of more C–S–H gel, which is primarily meant for strength development in cementitious materials. (b) The high surface area and two-dimensional structure of GO contribute to filling micro-pores, thus reducing porosity and enhancing the density of the concrete. A denser microstructure directly translates to improved mechanical performance. (c) GO sheets possess excellent tensile strength and flexibility. They contribute to bridging micro-cracks during the early stages of hydration, delaying crack propagation and thus improving the compressive strength over time. (d) The functional groups containing oxygen present on the surface of GO interact chemically with hydration products, enhancing the interfacial transition zone (ITZ), which is typically the weakest zone in conventional concrete.

For all mixes, compressive strength enhances steadily from 7 to 28 days, which aligns with the typical hydration process. However, the GO-modified samples show a more pronounced rate of strength gain. This suggests that GO not only enhances the initial nucleation but also contributes to continued microstructural refinement and densification throughout the curing period.

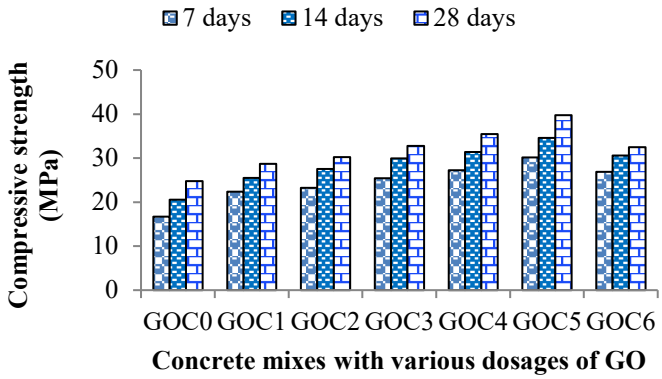

Fig. 1. Compressive strength of normal and GO reinforced concrete

Split tensile strength

Figure 2 presents the details of the split tensile strength of concrete samples containing varying percentages of graphene oxide at 7, 14, and 28 days**.** A control mix without GO (GOC0) was compared against mixes incorporating 0.01 to 0.05% and 0.1% GO by weight of cement. The split tensile strength of all GO-incorporated mixes exhibited a noticeable enhancement over the control mix across all curing periods. The percentage increase in strength of GO modified mixtures (GOC1, GOC2, GOC3, GOC4, GOC5, and GOC6) at 28 days relative to the control mix (GOC0) is found to be nearly 14, 27, 55, 77, 109, and 63%. It is seen from the results that the inclusion of GO significantly enhances split tensile strength, with the most pronounced improvement observed at 0.05% GO addition, where the 28-day strength is enhanced by approximately 109% compared to the normal mixture. At 0.1 % GO dosage, the increasing trend of strength development drops, which may be due to GO agglomeration**,** reduced dispersion, and microvoid formation. The trend of strength gain with GO addition was also consistently reflected at 7 and 14 days, indicating the positive influence of GO from the early stages of curing.

The observed improvement in split tensile strength with increasing GO content can be attributed to the following mechanisms: (i) Graphene oxide particles possess an ultrafine structure with a high surface area and can effectively fill microvoids within the cement matrix. This densification leads to a more refined and less porous microstructure, thereby enhancing tensile strength. (b)The sheet-like morphology and excellent mechanical properties of GO enable it to act as a nano-reinforcement that bridges microcracks and restricts their propagation under tensile stresses. This mechanism significantly contributes to the development of tensile strength. **(c)** GO contains abundant oxygenated functional groups (hydroxyl, carboxyl, and epoxy) that promote nucleation sites for C-S-H gel during hydration. This interaction refines the microstructure of the ITZ (Interfacial transition zone) and enhances the bond between the paste and aggregates, leading to higher tensile performance. (d)The incorporation of GO improves the interfacial adhesion within the cementitious matrix, enhancing the stress transfer capacity across micro-defects. As a result, the concrete exhibits higher tensile strength when subjected to splitting loads. While all GO dosages

positively influenced strength, the 0.05% addition (GOC5) yielded the maximum benefit in this study. This suggests that at this concentration, the dispersion of GO is optimal for promoting microstructural improvements and mechanical reinforcement.

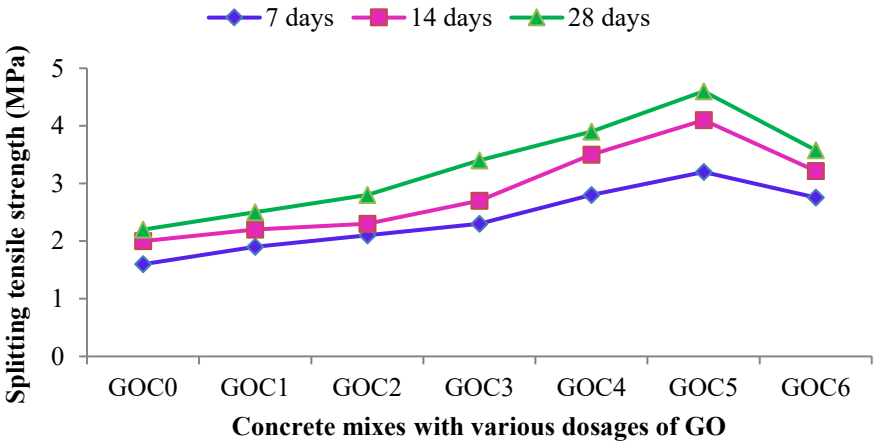

Fig. 2. Splitting tensile strength of normal and GO reinforced concrete

Flexural strength

The results of the flexural strength tests for PSC concrete with and without the addition of graphene oxide at different percentages (0.01 to 0.05% and 0.1% GO by weight of cement) are presented in Figure 3**.** The flexural strengths were recorded at 7, 14, and 28 days of curing. A comparative analysis of the data reveals a consistent improvement in the flexural strength of concrete with the incorporation of GO compared to the normal sample (PSC without GO). The increases in flexural strength at 28 days relative to the normal mix are found to be 9-39%. The addition of GO significantly enhanced the flexural strength over the entire curing period (7, 14, and 28 days). The improvement is progressive with the increase in GO dosage, reaching the highest strength at 0.05% GO. Beyond this, at 0.1 % content of GO, the ascending trend breaks, but the results remain more than normal concrete.

Graphene oxide, due to its high surface area and chemical functionality (oxygen-containing groups like hydroxyl, carboxyl, and epoxy groups), serves as an effective nucleation site for the growth of cement hydration products, mainly C-S-H gel. This enhanced nucleation accelerates the hydration process and leads to a denser microstructure, improving mechanical properties. The incorporation of GO promotes a more refined and compact microstructure by filling microvoids and reducing porosity. This leads to reduced crack propagation paths under flexural loads, thereby enhancing flexural strength. Graphene oxide sheets possess excellent mechanical properties and can bridge microcracks within the cement matrix. The bridging action of GO sheets across cracks impedes crack widening and propagation, contributing significantly to the observed increase in flexural strength. The functional groups of oxygen on the GO surface improve the interfacial bonding between the cement hydration products and the GO sheets, leading to better stress transfer across the matrix, further enhancing flexural performance. The results indicate a proportional

relationship between GO content and strength improvement up to 0.05%. The increase from 5.4 N/mm² (control) to 7.5 N/mm² (0.05% GO) represents a substantial 38.89% improvement in 28-day flexural strength.

The rate of strength gain is more pronounced at early ages (7 and 14 days) in GO-incorporated samples, indicating accelerated hydration kinetics due to GO's nucleation effect. At 0.05% GO, the flexural strength reached a maximum, suggesting this dosage as an optimum limit within the tested range for achieving significant mechanical improvement without potential risks of agglomeration or workability loss, which typically occur at higher dosages.

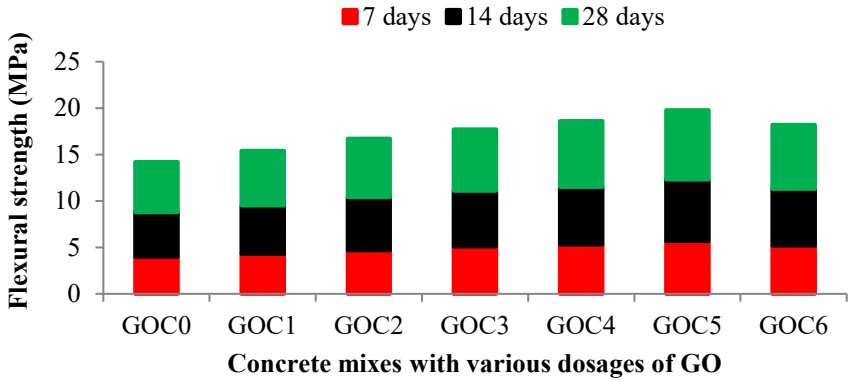

Fig. 3. Flexural strength of normal and GO reinforced concrete

Scanning electron microscopy

Figure 4 (A) displays the microstructure of normal cement concrete analyzed using a Scanning Electron Microscope (SEM) at 5000x magnification. The dense regions observed are likely composed of C-S-H, the important binding phase formed during cement hydration. These regions exhibit a fine, irregularly layered, or fibrous morphology. Sharp-edged particles embedded in the matrix correspond to unhydrated or partially hydrated cement grains. Plate-like structures, visible in certain areas, are likely $Ca(OH)_2$. The image also reveals voids and microcracks, which could be attributed to inherent porosity or shrinkage during hydration. Additionally, scattered debris and aggregate fines are present, possibly originating from the fracture surface or incomplete mixing during mortar preparation. The interfacial transition zone appears to be weak.

Fig. 4 (B) illustrates the SEM image of the cement composite modified with 0.05% GO. A comparative morphological analysis between normal cement concrete and GO-modified cement mixture reveals notable differences. The GO-modified mortar exhibits distinct sheet-like structures, characterized by wrinkled or folded layers of graphene oxide dispersed throughout the matrix. This incorporation results in improved matrix uniformity, with fewer visible microcracks compared to the normal mortar. The GO sheets appear to interact with hydration products, significantly enhancing the compactness of the microstructure and modifying the interfacial transition zone. Additionally, the reduced presence of unhydrated cement particles indicates improved hydration efficiency, likely driven by GO's high surface area and

active chemical functional groups, which facilitate hydration reactions. The interconnected GO sheets seem to bridge microcracks and pores, contributing to a denser and more refined microstructure. This transformation reduces voids within the mortar, suggesting a lower water sorption potential.

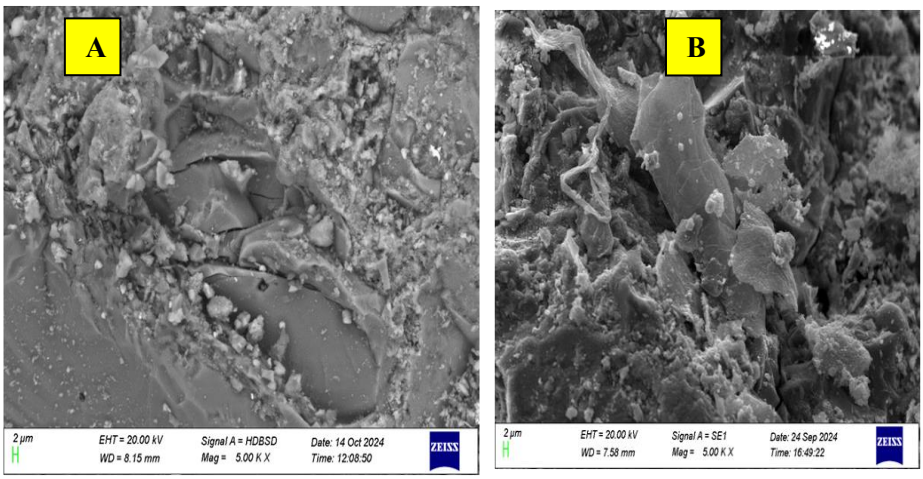

Fig. 4. SEM images of normal and GO-modified mixes

Energy dispersive X-ray spectroscopy

The EDX analysis results, as shown in Fig. 5 and Table 6, provide a detailed overview of the elemental composition of normal cement concrete. The spectrum reveals prominent peaks corresponding to oxygen (O), silicon (Si), and calcium (Ca), which are the dominant elements in the matrix. The high percentages of these elements confirm the prevalence of oxides, essential for hydration reactions and the development of strength in the cement composite. Aluminum (Al) and iron (Fe), also detected, play a key role in forming the C_3A and C_4AF phases, which significantly influence workability and sulfate resistance. Trace elements such as magnesium (Mg), sulfur (S), and potassium (K) are present in small quantities, likely originating from raw materials. Notably, the higher error margins for trace elements are attributed to their low concentrations, highlighting the limitations of EDX in detecting elements with low-intensity peaks. Overall, the findings align well with the expected chemical composition of normal cement mortar.

Table 6: EDx results of normal cement concrete

Element	Weight %	MDL	Atomic %	Error %
O K	54.9	0.32	70.4	10.6
Mg K	1.0	0.17	0.8	14.0
Al K	1.4	0.14	1.1	10.5
Si K	27.1	0.13	19.8	5.4
S K	1.0	0.18	0.7	17.4
K K	0.4	0.19	0.2	28.3
Ca K	12.7	0.27	6.5	3.9
Fe K	1.5	0.35	0.5	14.0

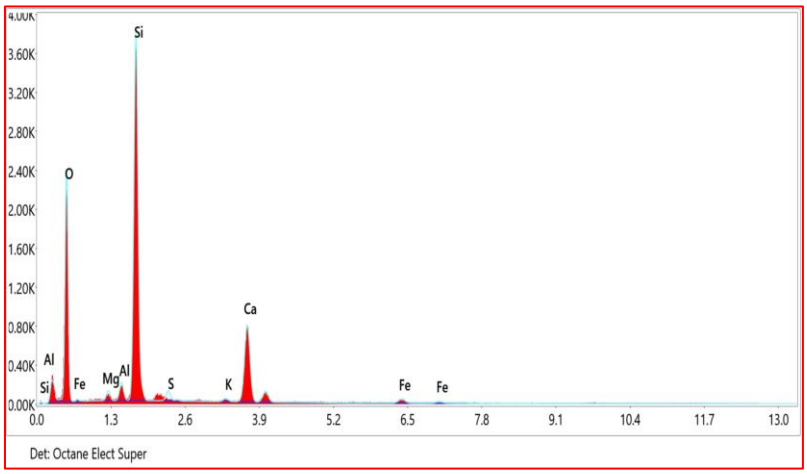

Fig. 5. EDX image of normal cement concrete

Table 7 and Figure 6 present the EDX analysis of the cement concrete sample, which contains 0.05% graphene oxide. Comparing the results with the normal concrete sample, a notable reduction in oxygen content by nearly 12% was observed. This decrease is likely attributed to enhanced silicate phases or reduced porosity in the modified mortar. Additionally, the silicon content showed a significant increase of 64.57%, indicating improved silicate polymerization facilitated by the interaction with graphene oxide. Conversely, calcium content exhibited a substantial reduction of 89.8%, suggesting decreased portlandite formation. This reduction likely contributes to a denser microstructure with enhanced chemical resistance. The presence of sodium in the modified mortar, which may have originated as an impurity or by-product from the graphene oxide, was also detected. Furthermore, an increase in sulphur content points to the formation of additional sulphate compounds, potentially influencing the sulphate resistance properties of the material.

The EDX analysis was used primarily as a qualitative microstructural support tool rather than a quantitative indicator of bulk hydration chemistry. The observed variations in elemental weight percentages between control and GO-modified samples reflect localized compositional differences influenced by sampling location and exposed phases. Therefore, the EDX results are interpreted cautiously and in conjunction with SEM morphology and XRD phase evolution. The enhanced C–S–H development and reduced portlandite formation inferred in this study are mainly supported by XRD patterns and mechanical performance, while EDX trends are considered indicative of localized microstructural refinement rather than absolute chemical transformation.

Table 7: EDX results of graphene oxide-modified cement concrete

Element	Weight %	MDL	Atomic %	Error %
O K	48.5	0.45	62.8	11.0
Na K	0.7	0.44	0.7	41.7
Mg K	0.7	0.27	0.6	26.4
Al K	1.1	0.23	0.8	17.6
Si K	44.6	0.21	32.9	5.3
S K	1.4	0.34	0.9	22.6
Ca K	1.3	0.42	0.7	22.9
Fe K	1.5	0.52	0.6	19.5

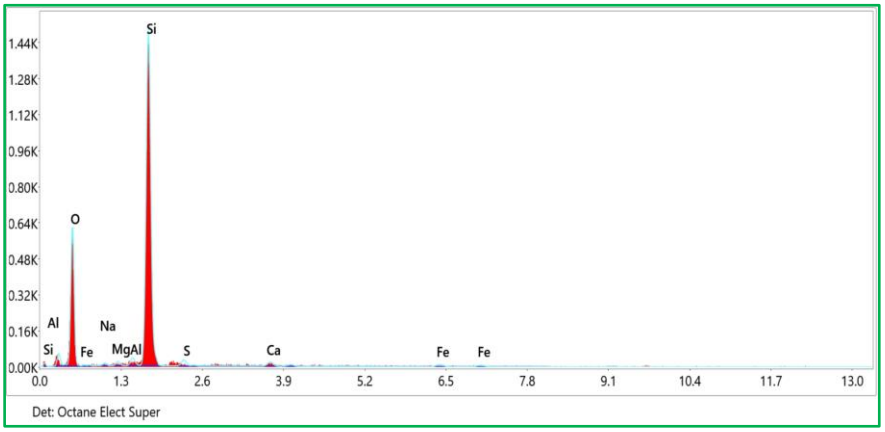

Fig. 6. EDX image of graphene oxide-modified cement concrete

X-ray diffraction

The XRD patterns of the graphene oxide–modified cement concrete mixes (Fig. 7) reveal distinct changes in phase assemblage with increasing GO content, indicating notable microstructural evolution during hydration. In the control mix (COC0), the dominant crystalline phases are quartz (Q), portlandite (P), and calcite (C), which correspond to typical constituents of Portland slag cement systems. With the incorporation of GO at low dosages (COC1–COC3), additional peaks corresponding to ettringite (E) and tobermorite-like calcium silicate hydrate (T) become more prominent, suggesting that GO facilitates early-age nucleation and growth of hydration products. The increased intensity of ettringite and C–S–H (tobermorite) peaks in these mixes indicates enhanced sulfate–aluminate hydration and accelerated silicate polymerisation, likely due to the high surface functionality and oxygen-containing groups on GO that act as heterogeneous nucleation sites. As GO dosage increases further (COC4–COC6), the persistence of strong calcite and C–S–H peaks, along with a moderated presence of portlandite, suggests more efficient consumption of $Ca(OH)_2$ through pozzolanic interactions and carbonation-driven stabilization. The consistent quartz reflections across all mixes confirm its inert filler role, serving as a baseline reference. Overall, the progressive refinement of the crystalline phases,

particularly the increased formation of ettringite and tobermorite, demonstrates that GO addition not only accelerates hydration but also promotes a denser and more integrated microstructure. These mineralogical transformations are consistent with the enhanced mechanical and durability performance observed in GO-modified systems, reflecting the synergistic role of GO as a microstructural regulator and hydration promoter in PSC-based concretes.

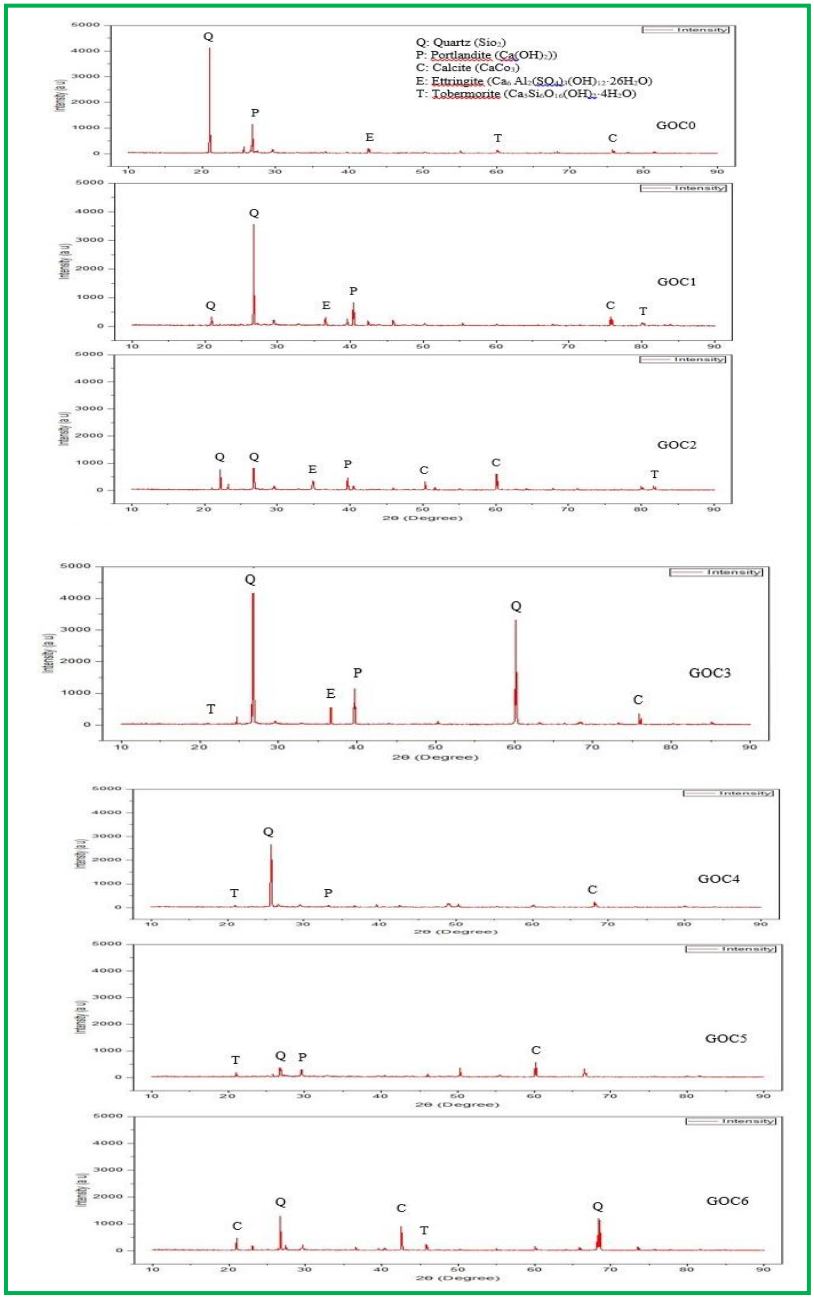

Fig. 7. XRD images of graphene oxide-modified and non-modified cement concrete

Acid Attack Test

The results presented in Figure 8 were derived from the average percentage strength loss of the specimens after 28 days of immersion in a 1% sulfuric acid (H_2SO_4) solution. The control mix recorded a strength loss of 5.78%, whereas the GO-modified mixes exhibited substantially lower strength loss, ranging from 3.85% to 3.15% for GO dosages between 0.01 and 0.05%. This corresponds to an improvement of approximately 33–46% compared to the control. However, the specimen containing 0.10% GO experienced a slightly higher strength loss of 3.21%, which is about 2% greater than the loss observed in the 0.05% GO sample. This marginal decline in performance at higher GO content suggests that excess GO may hinder the material's resistance to acid attack. Based on these observations, the optimal performance was achieved at a GO dosage of 0.05%.

The improved acid resistance observed in the GO-modified PSC concrete can be attributed to the synergistic physical and chemical interactions between graphene oxide and the hydration products of PSC. PSC contains a significant proportion of latent hydraulic slag, which contributes to the formation of additional C–S–H gel through secondary pozzolanic reactions. This results in a denser and more refined microstructure. When GO is incorporated in controlled dosages (0.01–0.05%), its two-dimensional sheet-like morphology and high surface area enable it to act as a nucleation site for C–S–H growth. This promotes accelerated hydration, refinement of pore size distribution, and improved particle packing within the cement matrix. Moreover, the abundant oxygen-containing functional groups on GO, such as hydroxyl, epoxide, and carboxyl groups, form chemical interactions with calcium ions released during hydration. These interactions enhance GO's dispersion and strengthen the interfacial bonding between GO sheets and C–S–H phases, further reducing microstructural defects that could otherwise facilitate acid penetration.

The reduced strength loss of GO-modified samples under sulfuric acid exposure can therefore be explained by this denser and chemically stable microstructure. The protective C–S–H network formed in PSC is inherently more resistant to acidic environments than calcium hydroxide (CH), which is more susceptible to leaching. Because PSC has lower CH content and higher C–S–H content, its vulnerability to acid dissolution is comparatively lower; the presence of GO reinforces this advantage by creating tortuous diffusion paths that slow down the ingress of aggressive ions. The sharp improvement, 33–46% reduction in strength loss at GO dosages up to 0.05%, reflects an optimal enhancement of matrix density and bonding. However, the slight decline in acid resistance at 0.10% GO suggests that higher GO content leads to agglomeration due to insufficient dispersion. Agglomerated GO clusters do not contribute effectively to hydration and may even introduce weak zones, microvoids, or discontinuities in the matrix. Such defects can provide preferential pathways for sulfuric acid attack, resulting in the marginally higher weight loss observed in the 0.10% GO sample. The results clearly indicate that the combined physicochemical effects of PSC hydration and optimally dispersed GO significantly enhance acid resistance, with 0.05% GO emerging as the most effective dosage for achieving maximum durability in sulfuric acid environments.

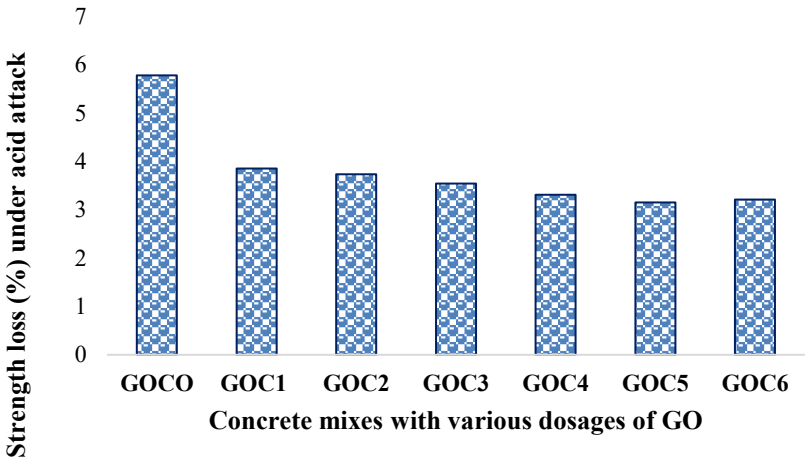

Fig. 8. Strength loss (%) after 28 days of acid exposure

Sulphate Attack Test

The results illustrated in Figure 9 indicate that exposure to a 1% $MgSO_4$ solution for 28 days led to measurable strength degradation in all mixes, though the extent of deterioration varied significantly with the addition of GO. The control mix (GOC0) exhibited a strength loss of 5.15%, whereas mixes containing 0.01–0.05% GO demonstrated substantially reduced losses, ranging from 4.68% down to 3.60%. These reductions correspond to approximately 9–30% improvement in sulphate resistance relative to the control. Nevertheless, when the GO dosage was increased to 0.10%, the strength loss rose slightly to 3.95%, which is about 10% higher than the loss recorded for the 0.05% GO mix. This indicates that while low-to-moderate GO content enhances durability, excessive GO may disrupt the microstructure or hydration balance, resulting in marginally reduced performance compared to the optimal dosage.

From a scientific standpoint, the enhanced sulphate resistance imparted by GO at lower dosages can be attributed to its influence on both the physical and chemical aspects of the cementitious matrix. First, GO's high surface area and functional groups facilitate improved nucleation sites for the formation of C–S–H gel, leading to a denser and more refined pore structure. This reduced permeability limits the ingress of sulphate ions, thereby mitigating the extent of deleterious reactions such as the formation of expansive ettringite and gypsum. Additionally, the oxygen-containing functional groups on GO can promote better interfacial bonding within the matrix, strengthening the microstructural integrity and making it more resistant to chemical attack.

However, when GO is incorporated beyond the optimal level, particle agglomeration becomes more likely, which can introduce weak zones or microvoids. These defects counteract the benefits of densification and may allow easier penetration of

aggressive ions. Moreover, excessive GO may interfere with normal cement hydration by adsorbing too much water or disrupting crystal growth, resulting in incomplete or irregular formation of hydration products. This explains the slight decline in performance observed for the 0.10% GO mix. The findings demonstrate that GO enhances sulphate resistance primarily through pore refinement, improved matrix densification, and strengthened interfacial bonding—but only when used within an optimal dosage range, with 0.05% identified as the most effective level for resisting magnesium sulphate attack in the present study.

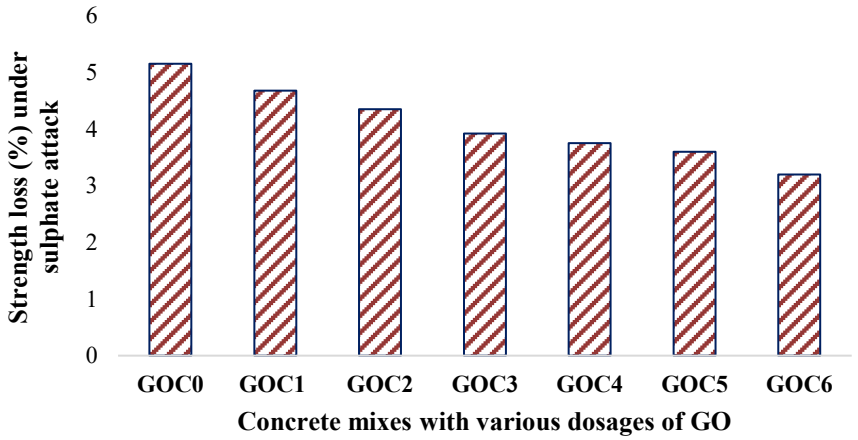

Fig. 9. Strength loss (%) after 28 days of sulphate exposure Future scope of work

This study primarily focused on the compressive, tensile, and flexural strength of GO-modified slag cement concrete. Future investigations should include fracture energy and toughness evaluation to fully capture the ductility and post-cracking behavior induced by graphene oxide. Similarly, the present study focused on acid and sulphate resistance characteristics of GO-modified concrete. Further study may be carried out concerning resistance to other aggressive environments. Future work may incorporate quantitative dispersion and rheological assessments to strengthen the mechanistic understanding.

Conflict of Interest:

There was no relevant conflict of interest regarding this paper.

References

I. Acharya, P. K., and S. K. Patro. “Acid Resistance, Sulphate Resistance and Strength Properties of Concrete Containing Ferrochrome Ash (FA) and Lime.” *Construction and Building Materials*, vol. 120, 2016, pp. 241–250, 10.1016/j.conbuildmat.2016.05.099.

II. Bureau of Indian Standards. *IS 10262: Concrete Mix Proportioning – Guidelines*. 2nd rev., BIS, 2019, New Delhi, India.

III. Bureau of Indian Standards. *IS 383: Coarse and Fine Aggregate for Concrete – Specification*. 3rd rev., BIS, 2016, New Delhi, India.

IV. Bureau of Indian Standards. *IS 455: Portland Slag Cement – Specification*. 5th rev., BIS, 2015, New Delhi, India.

V. Bureau of Indian Standards. *IS 516 (Part 1/Section 1): Hardened Concrete – Methods of Test: Compressive, Flexural and Split Tensile Strength*. BIS, 2021, New Delhi, India.

VI. Bureau of Indian Standards. *IS 516 (Part 2/Section 2): Hardened Concrete – Methods of Test: Initial Surface Absorption*. BIS, 2020, New Delhi, India.

VII. Bureau of Indian Standards. *IS 5816: Method of Test for Splitting Tensile Strength of Concrete*. BIS, 1999, reviewed 2018, New Delhi, India.

VIII. Chaipanich, A., et al. "Compressive Strength and Microstructure of Carbon Nanotubes–Fly Ash Cement Composites." *Materials Science and Engineering A*, vol. 527, no. 4–5, 2010, pp. 1063–1067.

IX. Chuah, S., et al. "Nano Reinforced Cement and Concrete Composites and New Perspective from Graphene Oxide." *Construction and Building Materials*, vol. 73, 2014, pp. 113–124.

X. Cwirzen, A., K. Habermehl-Cwirzen, and V. Penttala. "Surface Decoration of Carbon Nanotubes and Mechanical Properties of Cement/Carbon Nanotube Composites." *Advances in Cement Research*, vol. 20, no. 2, 2008, pp. 65–73.

XI. Fu, K., et al. "Defunctionalization of Functionalized Carbon Nanotubes." *Nano Letters*, vol. 1, no. 8, 2001, pp. 439–441.

XII. Gaitero, J. J., I. Campillo, and A. Guerrero. "Reduction of the Calcium Leaching Rate of Cement Paste by Addition of Silica Nanoparticles." *Cement and Concrete Research*, vol. 38, no. 8–9, 2008, pp. 1112–1118.

XIII. Gholampour, A., et al. "From Graphene Oxide to Reduced Graphene Oxide: Impact on the Physiochemical and Mechanical Properties of Graphene-Cement Composites." *ACS Applied Materials & Interfaces*, vol. 9, no. 49, 2017, pp. 43275–43286.

XIV. Kang, D., et al. "Experimental Study on Mechanical Strength of GO–Cement Composites." *Construction and Building Materials*, vol. 131, 2017, pp. 303–308.

XV. Keyvani, A. *Huge Opportunities for Industry of Nanofibrous Concrete Technology*. PhD thesis, Azarbaijan University of Tarbiat Moallem, 2007.

XVI. Konsta-Gdoutos, M. S., Z. S. Metaxa, and S. P. Shah. "Highly Dispersed Carbon Nanotube Reinforced Cement-Based Materials." *Cement and Concrete Research*, vol. 40, no. 7, 2010, pp. 1052–1059.

XVII. Li, G. Y., P. M. Wang, and X. Zhao. "Mechanical Behavior and Microstructure of Cement Composites Incorporating Surface-Treated Multi-Walled Carbon Nanotubes." *Carbon*, vol. 43, no. 6, 2005, pp. 1239–1245.

XVIII. Li, G. Y., P. M. Wang, and X. Zhao. "Pressure-Sensitive Properties and Microstructure of Carbon Nanotube Reinforced Cement Composites." *Cement and Concrete Composites*, vol. 29, no. 5, 2007, pp. 377–382.

XIX. Li, H., et al. "Microstructure of Cement Mortar with Nanoparticles." *Composites Part B: Engineering*, vol. 35, no. 2, 2004, pp. 185–189.

XX. Liu, J., et al. "Fracture Toughness Improvement of Multi-Wall Carbon Nanotubes/Graphene Sheets Reinforced Cement Paste." *Construction and Building Materials*, vol. 200, 2019, pp. 530–538, 10.1016/j.conbuildmat.2018.12.141.

XXI. Lv, S., et al. "Effect of GO Nanosheets on Shapes of Cement Hydration Crystals and Their Formation Process." *Construction and Building Materials*, vol. 64, 2014, pp. 231–239.

XXII. Lv, S., et al. "Effect of Graphene Oxide Nanosheets on Microstructure and Mechanical Properties of Cement Composites." *Construction and Building Materials*, vol. 49, 2013, pp. 121–127.

XXIII. Lv, S. H., et al. "Study of Graphene Oxide Reinforced Toughened Cementitious Composites." *Functional Materials*, vol. 44, no. 15, 2013, pp. 2227–2231.

XXIV. Lv, S. H., et al. "Toughening Effect and Mechanism of Graphene Oxide Nanoflakes on Cementitious Composites." *Journal of Composite Materials*, vol. 31, no. 3, 2014, pp. 644–652.

XXV. Makar, J. "The Effect of SWCNT and Other Nanomaterials on Cement Hydration and Reinforcement." *Nanotechnology in Civil Infrastructure*, edited by K. Gopalakrishnan et al., Springer, 2011, pp. 103–130.

XXVI. Nasibulin, A. G., et al. "A Novel Cement-Based Hybrid Material." *New Journal of Physics*, vol. 11, 2009, article 023013.

XXVII. Pan, Z., et al. "Mechanical Properties and Microstructure of a Graphene Oxide–Cement Composite." *Cement and Concrete Composites*, vol. 58, 2015, pp. 140–147.

XXVIII. Sáez de Ibarra, Y., et al. "Atomic Force Microscopy and Nanoindentation of Cement Pastes with Nanotube Dispersions." *Physica Status Solidi A*, vol. 203, no. 6, 2006, pp. 1076–1081.

XXIX. Sanchez, F., and C. Ince. "Microstructure and Macroscopic Properties of Hybrid Carbon Nanofiber/Silica Fume Cement Composites." *Composites Science and Technology*, vol. 69, no. 7–8, 2009, pp. 1310–1318.

XXX. Sedaghat, A., et al. "Investigation of Physical Properties of Graphene Cement Composite for Structural Applications." *Open Journal of Composite Materials*, vol. 4, no. 1, 2014, pp. 12–21.

XXXI. Shah, S. P., et al. *Highly Dispersed Carbon Nanotubes Reinforced Cement-Based Materials*. United States Patent Application Publication No. US2009/0229494 A1, 2009.

XXXII. Shang, Y., et al. "Effect of Graphene Oxide on the Rheological Properties of Cement Pastes." *Construction and Building Materials*, vol. 96, 2015, pp. 20–28.

XXXIII. Wang, M., et al. "Study on the Three-Dimensional Mechanism of Graphene Oxide Nanosheets Modified Cement." *Construction and Building Materials*, vol. 126, 2016, pp. 730–739.

XXXIV. Wang, Z. M., and H. L. Zhang. "Study on the Mechanical Properties of Graphene Oxide Nanosheet Reinforced Cement-Based Composites." *Industrial Buildings*, vol. 51, no. 2, 2021, pp. 153–161.